3.1. Methodology used

A flowchart depicting the methodology adopted for the present study is shown below (Fig. 3.1)

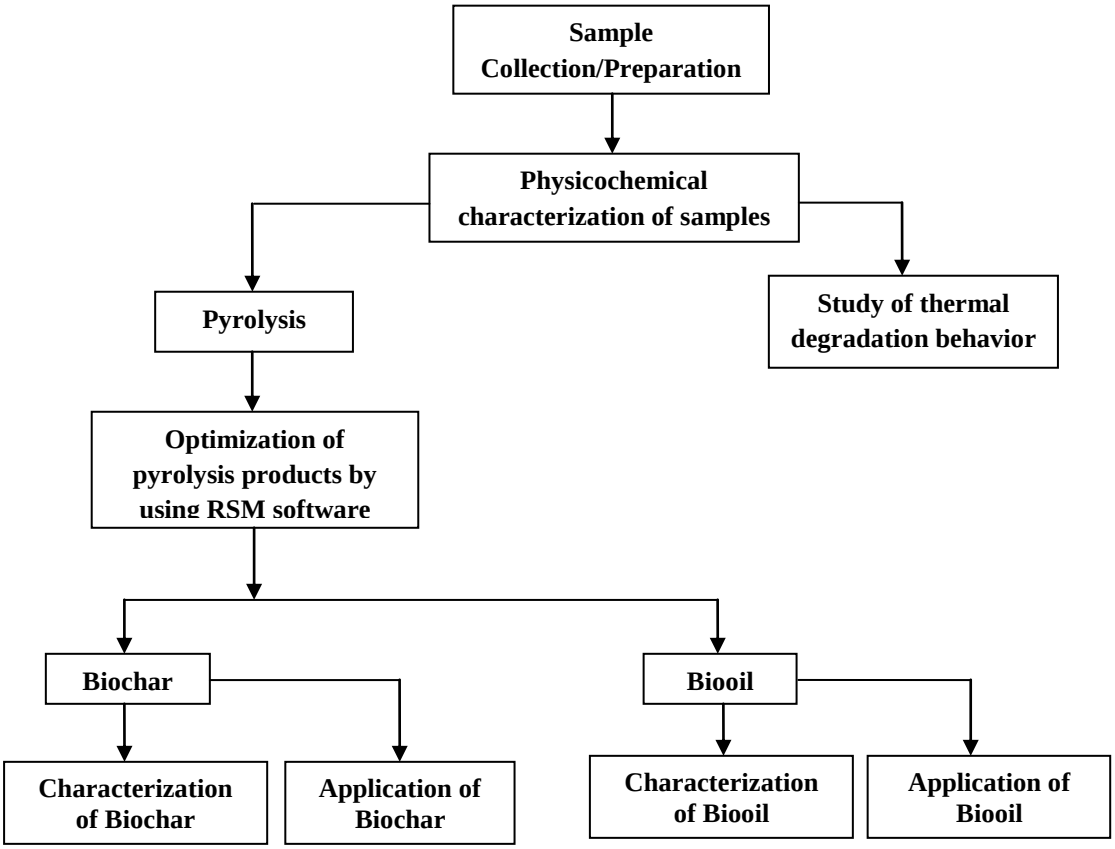

Fig. 3.1: Flowchart of methodology adopted for the present study

3.2. Materials

The feedstocks used in the present study were seed covers of two non-edible oil bearing seeds – *Mesua ferrea* and *Pongamia glabra.*

3.2.1. Mesua ferrea

Mesua ferrea commonly known as Nahar (in Assamese) is widely available in forest areas and also grown under social forestry as an ornamental tree due to its graceful shape. It is one of the hardest trees of north-east India. Timbers are used in railway sleepers, construction of houses, furniture and cart wheels etc. This tree is particularly found in upper Assam, lower Nagaland, Darrang district and North Cashar Hills. *Mesua ferrea* produces high-oil content seeds (58–75 wt.%). It is estimated that more than 10 million kilogram of *Mesua ferrea* seeds are produced annually in the Assam [1]. Flowers and leaves have snake repellent properties. *Mesua ferrea* seed and seed covers are shown in Fig. 3.2.

Fig. 3.2: *Mesua ferrea* seed and seed cover

3.2.2. Pongamia glabra

Pongamia glabra commonly known as Koroch (in Assamese) is a drought resistant, semi-deciduous, nitrogen fixing leguminous tree found in tropical parts of Asia including parts of India, China, Japan, Malaysia, and Australia. The tree has excellent medicinal properties. It is commonly used as a fuel. Its wood is susceptible to insect attack, and therefore, not considered as quality timber. It has been used as lamp oil, in leather tanning, in soap making, and as a lubricant for thousands of years [2]. High seed yielding tree (900-9000 kg seed/ha/year) and maximum oil production

(whole seed 33% and kernel 39%) [3]. *Pongamia glabra* seed and seed cover are shown in Fig 3.3.

Fig. 3.3: *Pongamia glabra* seed and seed cover

3.2.3. Scenedesmus dimorphus

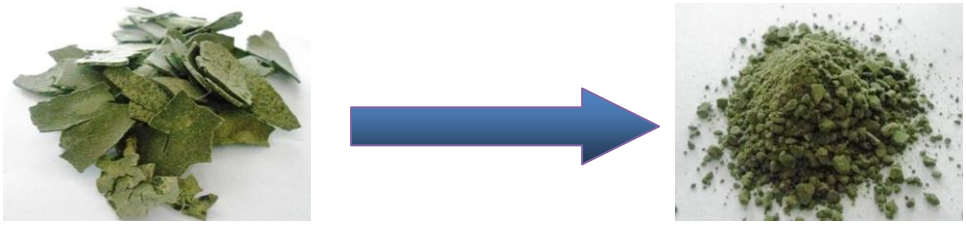

Fig. 3.4: Dried *Scenedesmus dimorphus*

Scenedesmus dimorphus is freshwater unicellular green algae in the class Chlorophyceae. Microalgae are fast growing biological systems which are capable of fixing high amount of carbon dioxide through photosynthesis to produce biomass. Micro algae have several advantages, including higher photosynthetic efficiency as well as higher growth rates and higher biomass production compared to other energy crops. Among microalgae, *Scenedesmus* genus has the most desirable features for efficient and economic combination of CO_2 fixation, wastewater treatment, and lipid synthesis toward biodiesel production. Recently, it has drawn attention as commercially valuable source for a wide spectrum of compounds such as; high quality protein, B12, C and E vitamins, other bioactive chemicals, long chain polyunsaturated fatty acids and phenolic compounds. *Scenedesmus dimorphus* seems to be the ideal species, due to its good ability to grow and tolerate different environmental conditions [4]. Dried *Scenedesmus dimorphus* are shown in Fig 3.4.

M. ferrea and *P. glabra* seed covers (MFSC and PGSC) were collected from the Biofuel Laboratory, Department of Energy, Tezpur University, India. Dried *S. dimorphus* sample was obtained from Defense Research Laboratory, Tezpur, India. All the three samples were crushed in a pulverizer and allowed to pass through 0.2 mm (70 mesh) sieve size (as per TAPPI T257 Om-85 methods). The ground samples were then oven dried at 60 ºC for over-night and then kept in desiccators for further analysis and pyrolysis experiment.

3.3. Proximate analysis

3.3.1. Determination of Moisture content

Moisture content of all the samples was determined according to the ASTM D 3173. The collected samples were weighed initially and then the samples were taken in an aluminum container and dried in an oven at 105 ± 3 ºC. The samples were kept in the oven until a constant weighed was reached. For each sample, the experiment was conducted in triplicate and the mean value was reported. The moisture content was determined by using the following equation:

$$Moisture\ content\ (\%) = \frac{Initial\ weight - Oven\ dry\ weight}{Initial\ weight} \times 100$$

3.3.2. Determination of ash content

Ash content was determined by using ASTM D 3174 method. At first, an empty 25 ml silica crucible was heated in a muffle furnace at 575 ± 25 ºC for 15 min and then allowed to cool in desiccators for 45 min and then weighed accurately. Oven dried biomass samples under investigation were weighed and transferred into the crucible and kept in a muffle furnace at 575 ± 25 ºC to ignite for a period of 3 hours or longer to burn away the carbon, completion of which was indicated by the absence of black particles. After cooling the furnace, crucible was removed and kept in desiccators and weighed accurately. For each sample, the estimation was done in triplicate and the mean value was reported. The percentage of ash content was calculated by using the following equation:

$$Ash\ content\ (\%) = \frac{Weight\ of\ ash}{Weight\ of\ sample} \times 100$$

3.3.3. Determination of volatile matter

Volatile matter of the samples was determined by ASTM 3175 method. A silica crucible of 10 ml capacity was heated in a preheated vertical tube furnace at 950 ºC for 2 min and then cooled in a desiccator for 15 min. The weight of the crucible was taken. The crucible was then filled with the ground oven dried samples and gross weight was taken. It was then heated again in the preheated furnace at 950 ºC for about 2 min. After that the crucible was removed from the furnace and cooled in air for 2 to 5 min and then cooled in a desiccator for 15 min. For each sample, the estimation was done in triplicate and the mean value was reported. The percentage of weight loss of the samples was reported as volatile matter and calculated as follows:

$$Volatile\ matter\ (\%) = \frac{Weight\ loss\ of\ dry\ sample}{Net\ weight\ of\ dry\ sample} \times 100$$

3.3.4. Determination of Fixed Carbon

Fixed carbon content of all samples was determined by simple calculation as given in ASTM Test No. D-271-48. The calculation was given as

$$Fixed\ carbon\ (on\ dry\ basis)(\%) = 100 - [Moisture\ (\%) + volatile\ matter\ (\%) + ash\ (\%)]$$

3.3.5. Higher heating value (HHV)

Gross calorific value or higher heating value was determined using an auto bomb calorimeter (5E-1AC/ML, Auto bomb calorimeter) according to ASTM D2015. About 1 g of oven dried sample was completely combusted in an adiabatic bomb containing 3.4 MPa pure oxygen under pressure.

3.4. Compositional analysis of the lignocellulosic biomass

Biomass samples were subjected to compositional analysis using the gravimetric method.

3.4.1. Extractives

Extractives were determined by using Soxhlet apparatus. Acetone (300 ml) was used as the solvent for extractive determination. 3 g (W_o, g) of dried raw biomass was loaded into the cellulose thimble. Residence times for the boiling and rising stages was carefully adjusted to 70 ºC and 25 min respectively on the heating mantle for a 4h run period. The sample was air dried for few minutes at room temperature. It was then dried at 105 ºC in an oven until a constant weight (W_1, g) was obtained. The extractives weight percent, % (w/w) was calculated by the equation given below [2]:

$$Extractives\ \%\ \left(\frac{w}{w}\right) = \left\{\frac{(W_0 - W_1)}{W_0}\right\} \times 100\%$$

3.4.2. Lignin

2g of dried extracted biomass was weighed in a glass test tube and sample was treated with ten times its weight with 72% H_2SO_4. The sample and acid were intimately mixed with a stirring rod, causing the sample to become completely disintegrated after a few hours. After hydrolysis has been allowed to proceed at room temperature for 16h, the acid was diluted to a concentration of 3 percent. The solution is then boiled under an air-cooled reflux condenser for 2h. The lignin was then filtered on a tarred sintered crucible (previously treated with acid), washed with hot water to make it free from acid. The crucible with lignin was then dried in an oven at 105 ± 3 ºC to constant weight. The dried crucible was then cooled in a desiccator and weight was recorded [5].

$$\text{Lignin, \%} = A \times 100/W$$

where, A = weight of lignin, g

W = oven-dry weight of test specimen, g

Holocellulose [Hemicellulose +Cellulose] % = 100 – Lignin%

3.5. Kinetic modeling

Pyrolysis of biomass can be represented by the following reaction scheme:

Biomass (solid) $\longrightarrow$ **Volatiles + Solid residues**

The conversion (α), is defined in terms of mass change in the biomass sample or the mass of volatile generated, is given by the following equation

$$\alpha = \frac{W_o - W_t}{W_0 - W_\infty} \quad (3.1)$$

Where, w_0, w_t and w_∞ are the initial, actual and final weights of the sample respectively [6]. The rate of decomposition is a function of temperature and conversion

$$\frac{d\alpha}{dt} = f(T, \alpha) \quad (3.2)$$

It is possible to rewrite the right hand side of equation (3.2) by using two functions, where the first is temperature dependent and the second one is a function of conversion.

$$\frac{d\alpha}{dt} = k(T)f(\alpha) \quad (3.3)$$

The temperature dependent function k(T) in equation (3.3) is usually expressed by Arrhenius equation

$$k(T) = A \exp\left(\frac{-E}{RT}\right) \quad (3.4)$$

Where, A is the pre-exponential factor, E is the activation energy and R is the gas constant.

The rate equation can be written as,

$$\left(\frac{d\alpha}{dt}\right) = A \exp\left(\frac{-E}{RT}\right) f(\alpha) \quad (3.5)$$

For non-isothermal condition the above equation can be written by introducing a heating rate: $\beta = \frac{dT}{dt}$

$$\beta\frac{d\alpha}{dT} = A \exp\left(\frac{-E}{RT}\right) f(\alpha) \quad (3.6)$$

For non-isothermal data, iso-conversional methods require performing a series of experiments at different temperature programs. The most popular methods are represented by the differential method of Friedman (FR) [7] and by the integral methods proposed by Flynn–Wall–Ozawa (FOW) [8-9] or Kissinger–Akahira–Sunose (KAS) [10-11]. These methods will be referred as conventional isoconversional methods that calculate activation energy (E_a) values at progressive values of conversion (α) [12].

3.5.1. Friedman method

The Friedman method is a differential method developed in 1964. It is called differential since the rate expression is evaluated in its differential form. The basic equation of Friedman's differential method is readily obtained by taking the logarithm of equation (3.5) [13].

$$\ln\left(\frac{d\alpha}{dt}\right) = \ln\left(\beta\frac{d\alpha}{dT}\right) = \ln[Af(\alpha)] - \frac{E}{RT} \qquad (3.7)$$

For any constant value of α, the effective activation energy can be obtained over a wide range of temperature by plotting $\ln\left(\beta\frac{d\alpha}{dT}\right)$ vs. $\frac{1}{T}$.

3.5.2. Flynn-Wall-Ozawa or FWO method

The activation energy (E_a) values for the degradation process were determined by the isoconversional Flynn–Wall-Ozawa (FWO) method. This method can be used for determination of the E_a values without any knowledge of the reaction mechanisms. The general form of FWO equation is given as

$$ln\beta = ln\frac{AE}{Rg(\alpha)} - 5.331 - 1.052\ \frac{E_a}{RT} \qquad (3.8)$$

Where, β is the heating rate, A is the pre-exponential factor, g(α) is a function of the conversion, E_a is the activation energy and R is the gas constant. Therefore, for different heating rates (β) and a given degree of conversion (α), a linear relationship is observed by plotting log β vs. 1/T, and the E_a is obtained from the slope of the straight line [14-15].

3.5.3. Kissinger-Akira-Sunnose or KAS method

Taking into account that the temperature is a function of time and that it is increasing with a constant heating rate, β, then β can be written as

$$\beta = \frac{dT}{dt} = \frac{dT}{d\alpha}\frac{d\alpha}{dt} \qquad (3.9)$$

Combining Eq. (3.5) and Eq. (3.9), and rearranging gives:

$$g(a) = \int_0^{\alpha} \frac{d\alpha}{f(\alpha)} = \int_0^{T} \frac{A}{\beta} e^{\frac{-E}{RT}} dT = \frac{AE}{\beta R}\int_x^{\infty} u^{-2}e^{-u}du = \frac{AE}{\beta R}P(x) \qquad (3.10)$$

Where, x = E_a/RT. The function P(x) has no exact solution. Thus Eq. (3.10) can be solved by numerical methods or approximations.

The Kissinger–Akahira–Sunose method (KAS) [12, 16] is obtained by introducing the approximation

$$P(x) = x^{-2}e^{-2}$$

into Eq. (3.10). After rearrangement, the expression becomes:

$$\ln\left(\frac{\beta}{T^2}\right) = \ln\left[\frac{AE}{Rg(\alpha)}\right] - \frac{E}{RT} \qquad (3.11)$$

In the plot of $\ln\frac{\beta}{T^2}$ vs. 1/T, slope gives -E_a/R where R is 8.314 J/mol K. By calculation in a conversion range from 0 to 1, activation energy for the progressing values of conversion can be calculated.

3.6. Pyrolysis experiment

The pyrolysis experiments were carried out in a fixed bed vertical, tubular reactor (length: 30 cm and internal diameter: 2.47 cm) made of quartz glass in which the temperature was controlled by Ni-Cr thermocouple placed in the center of electrical furnace (shown in Fig. 3.5). For each pyrolysis experiment, 10 g of the biomass sample was taken in the lab scale reactor at a bed height of 4 cm. The experiments were carried out with a temperature increment of 40 ºC/min to the final

temperature under constant flow rate of nitrogen at 100 ml/min. However, achievement of a higher heating rate (40 ºC/min) condition corresponds to slow pyrolysis tests. A condenser was attached at the outlet of the reactor to condense the vapors coming out of it where water was used as cooling medium. The condensed vapors were collected in a container as liquid product and non-condensable gases which were simply left out. The yields of liquid products and char were determined by weighing. The amount of gas was determined by difference. The liquid product consists of two phases: aqueous phase and organic phase (shown in Fig. 3.6). The aqueous phase was separated from the oil phase in a separating funnel using solvent, diethyl ether. The oil phase was then dried over anhydrous sodium sulfate, filtered and evaporated in a rotary evaporator at 30 ºC. Upon removal of diethyl ether, this fraction was weighted and termed as biooil which was then characterized by using various analytical techniques.

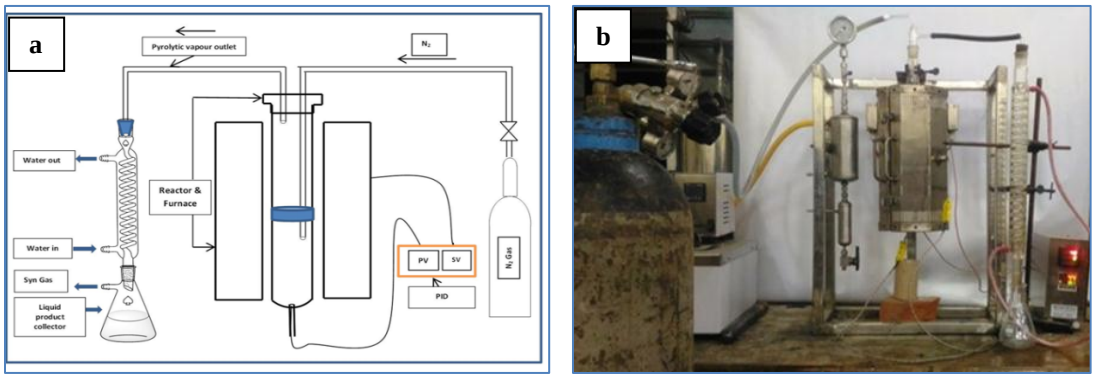

Fig. 3.5: Schematic (a) and pictorial (b) diagram of pyrolysis experimental setup

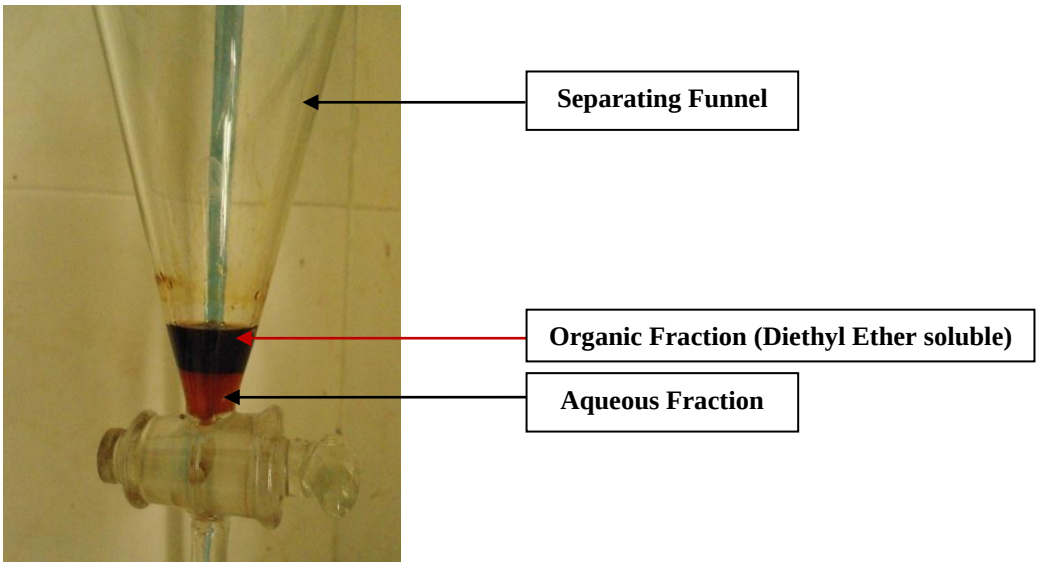

Fig. 3.6: Separation of Pyrolytic liquid

The following equations were used to calculate the product yields of pyrolysis experiments:

$$Oil\ yield\ (wt.\%) = \frac{W_{oil}}{W_{Biomass,db}} \times 100$$

$$Aqueous\ yield\ (wt.\%) = \frac{W_{Aqueous}}{W_{Biomass,db}} \times 100$$

$$Solid\ yield\ (wt.\%) = \frac{W_{Solid}}{W_{Biomass,db}} \times 100$$

$$Gas\ yield\ (wt.\%) = 100\% - Liquid\ yield\ (wt.\%) - Solid\ yield(wt.\%)$$

Where, W= weight and db= dry basis.

3.7. Response Surface Methodology (RSM)

The response surface methodology (RSM) was employed to evaluate the effect of reaction parameters, viz. temperature and heating rate on pyrolysis product distribution of biomass pyrolysis using central composite design (CCD) [17]. Design Expert software program, version 10.0.6. (Stat-Ease Inc., MN, USA), was used to develop the statistical model. The two design factors, temperature (A) and heating rate

(B) were taken as independent variables and the predicted responses as dependent variables. The experiments were conducted with three responses viz. yields of bio-oil, biochar and gas. In the present study, responses were studied within a certain range of temperature limit (350–650 ºC for MFSC and PGSC, and 300–600 ºC for *S. dimorphus*) and the range for heating rate from 10–40 ºC/min. Separate coded values and the natural values were obtained for each set of experiment. The number of total experiments (N) depends on the number of the design factors (here, n = 2) which can be expressed by the following equation

$$N = 2n + (2 \times n) + 5 = (2\times2) + (2\times2) + 5 = 13 \quad (3.12)$$

The CCD design analyzed for two variables consists of total 13 experimental runs with 4 factorial points, 4 axial points and 5 replicates at the center points.

After completion of the experiments, the response variables were fitted into a second-order model in order to correlate the response variable to the independent variable. The general form of the second degree polynomial equation is shown below

$$Y = b_0 + \sum_{i=1}^{k} b_i X_i + \sum_{i=1}^{k} b_{ij} X_i^2 + \sum_{i_{i>j}}^{k} \sum_{j}^{k} b_{ij} X_i X_j + e \quad (3.13)$$

where, i and j are the linear and quadratic coefficients, respectively, b is the regression coefficient, k is the number of factors studied and optimized in the experiment and e is the random error [17].

3.8. Fractionation of biooil

The different chemical classes of compounds present in the biooils were determined by fractionating using liquid column chromatography. The column having a diameter of 1.5 cm and length of 70 cm was packed with activated silica gel (70–230 mesh) up to 3/4 of the total volume and pretreated at 105 ºC for 2h (in absence of carrier gas) prior to use as reported elsewhere [19]. First the column was eluted with 500 ml n-hexane to obtain the n-hexane soluble fraction. After that the same column was eluated with toluene and ethyl acetate successively. At the end, the column was washed with methanol. Separate collecting bottles were used for eluent of each solvent. Collecting bottle was changed when the apparent color ribbon layer reached

the end of the column. Rotavapor was run by maintaining the temperature at 40 ºC and reduced pressure at 28 mmHg. The solvents remained after rotary evaporation was dried by using freeze dryer and then weights of sub-fractions were calculated and subjected to further analysis.

3.9. Instrumental Characterization

3.9.1. Elemental characterization

Ultimate analysis is performed to determine the elemental composition of the material. It was carried out by using a CHNS elemental analyzer (Euro EA elemental analyzer) which provides carbon, hydrogen, nitrogen, sulfur percentage. Oxygen percentage was determined by difference.

3.9.2. TGA analysis

A thermogravimetric analysis (TGA) of biomass degradation was carried using a TG 209F1 Libra analyzer (Netzsch, Germany). The experiments were conducted non-isothermally at three different heating rates of 10, 20 and 30 ºC/min, over the temperature range of 30–600 ºC. Pure nitrogen (99.99%) was used as carrier gas at a flow rate of 100 ml/min to provide an inert reaction environment. In each experiment, a sample weighing approximately 2–11 mg was used.

3.9.3. FTIR analysis

The FTIR (Fourier transforms infrared spectroscopy) spectrum of the sample was recorded on a Nicolet Impact I-410 model IR spectrometer at room temperature. A region of 4000–400 cm^{-1} and resolution of 4 cm^{-1} was used for analysis. FTIR spectra give the information about the presence of functional groups in a particular compound.

3.9.4. ^{1}H NMR

The ^{1}H NMR spectra of the biooil samples were recorded in a 400 MHz NMR spectrophotometer (JEOL, JNM ECS) by using deuterated chloroform ($CDCl_3$) as the internal standard and coupling constants were expressed in Hertz.

3.9.5. GC-MS

The biooil samples were analyzed by GC-MS (Perkin Elmer Claurus 600) equipped with TCD detector and DB-5ms column (60.0 × 250 µm). Helium (99.99%) was used as the carrier gas with constant flow of 1.0 ml/min. The oven temperature was programmed from 70 ºC (2 min) to 300 ºC at a heating rate of 10 ºC/min with a hold time of 10 min. A sample volume of 3 ml was injected. The MS was operated in an electron ionization mode and an m/z range from 24 to 624 was scanned. Details of the GC-MS analysis conditions are given in Table 3.1.

Table 3.1: GC-MS analyzer details

Instrument: Model	**Perkin Elmer Clarus 680 GC/600C MS**	
GC conditions:		
Column oven temperature Injection mode Injection temperature Split ratio Carrier gas	70 ºC Split 200 ºC 10:1 He	
Column oven temperature progress:		
Heating rate	Temperature	Hold time (min)
-	70 ºC	2
10 ºC/min	290 ºC	7 (31 min total)
Column: DB -5	60.0m x 250µm	
MS condition		
Ion source temperature	180 ºC	
Interface temperature	200 ºC	

3.9.6. Calorific value

Calorific value of a material is the amount of heat liberated when unit weight (1 g or 1 kg) of that material is burnt. It was determined by using a bomb calorimeter (5E-1AC/ML, Auto bomb calorimeter) according to ASTM D2015. In this process the sample was completely combusted in an adiabatic bomb containing 3.4 MPa pure Oxygen under pressure.

3.9.7. Determination of pH and Electrical Conductivity

pH values were measured by adding biochar to de-ionized water in a mass ratio of 1:20. The solution was then hand shaken and allowed to stand for 5 min

before measuring the pH with a pH meter (EUTECH Instruments pH 700). Electrical conductivity (EC) of biochars were measured with conductivity meter (Digital TDS/Conductivity Meter MK509) using the same solution as prepared for pH measurement. The purpose for measurement of pH was to understand how application of biochar can influence soil acidity. This is particularly important as the soil of north-east India is generally acidic in nature. EC values of biochar is significant as it is directly proportional to the amount of salt (ion) concentration present in biochar and is therefore, related to the buffering capacity and cation exchange capacity (CEC) of biochar.

3.9.8. SEM and EDX analysis

Scanning electron microscopy (JEOL JSM-6390 LV, Japan) coupled with energy dispersive X-ray spectroscopy (Oxford EDX) was used to examine surface morphology and elemental composition of solid samples. SEM images were taken with an acceleration voltage of 20 kV at different magnifications with resolution of 0.03 nm.

3.9.9. XRD analysis

X-ray diffraction (XRD) analysis (BRUKER AXS, Germany, D8Focus) was conducted on solid samples to identify possible crystalline structures and the powder X-ray was recorded on a Rigaku miniflex diffractometer (Cu-Kα radiation, λ= 1.5406 Å) in 2θ range of 10–70º at a scanning rate of 20º min .

3.9.10. Carbon sequestration potential

Carbon sequestration potential (CSP) can be considered as the final amount of carbon that is captured in the soil. CSP was calculated by subtracting carbon loss during pyrolysis from C present in the raw biomass and multiplying it by recalcitrance (R_{50}), where weight of the feedstock could be taken as M (g). R_{50} index was used to evaluate the thermal recalcitrance of biochar and was obtained from TGA analysis as proposed by Harvey et al. [18].

$$R_{50}, \text{ of biochar} = \frac{T\,(50)\ \text{biochar}}{T\,(50)\ \text{graphite}} \qquad (3.14)$$

where, $T_{50,\ biochar}$ and $T_{50,\ graphite}$ are the temperature at which 50% weight was lost by oxidation/volatilization of biochar and graphite, respectively in atmosphere, values were obtained from TG thermograph [20].

$$CS\ (\%) = \frac{M\ (g)\ \times \text{char yield}\ \%\ \times \text{carbon}\ \%\ \text{biochar} \times R\ (50)\text{index of biochar}}{M\ (g)\ \times \text{carbon}\ \%\ \text{of feedstock}} \qquad (3.15)$$

3.10. Application of biochar

3.10.1. Adsorption of cobalt (Co) metal by using biochar as adsorbent

All chemical reagents used in the present study were of analytical grade quality (Merck Specialties Private Limited). The stock solution of 5 mM Co was prepared by dissolving the prescribed amount of Cobalt nitrate hexahydrate ($Co(NO_3)_2 \cdot 6H_2O$) (AR) in a 0.01 M $NaNO_3$ solution. The experiment was conducted in 250 ml conical flasks by mixing 0.1 g of biochar with 25 ml of 0.01 M $NaNO_3$ (to adjust the ionic strength) solution containing 1, 2, 3, 4, and 5 mM Co. The pH inside the flasks was adjusted to 5.0 by adding small amounts of HNO_3 (1 M) or NaOH (1M) solutions [21-22]. The flasks were then placed on a shaking table (RELITECH) and agitated for a determined period of time (15, 20, 30, 60, 90 and 180 min) with 150 rpm at room temperature. After agitation, the mixtures were filtered using Whatman No. 42 filter paper. The filtrates were used for analyses using an Atomic Absorption Spectrometer (Thermo Scientific, UK, AAS-ICE 3500) to find the concentration of Co (II) ions. The data obtained were tested against the linear forms of Langmuir, Freundlich, Temkin, Dubinin-Radushkevich (D-R) and Harkins-Jura isotherms. In order to investigate the controlling mechanism of adsorption processes, the pseudo-first-order and pseudo-second order equations were applied.

3.10.2. Adsorption of cationic dyes by using biochar as adsorbent

Two cationic dyes Methylene Blue (MB) and Rhodamine B (RB) were selected as adsorbate for the present study. Various amounts of biomasses were incubated individually for adsorption of MB and RB from aqueous solutions (50 ppm). For optimum adsorption of MB, 30 g/L of biochar and for RB, 50 g/L of biochar were used (where, L stands for liter). The tubes were incubated at 28 ºC for 24h in a shaker at 60 rpm. Thereafter, the biomass was segregated by centrifugation

and the dye concentration in the supernatant was estimated using an atomic adsorption spectrophotometer (AAS, MultiScan Go, Thermo Scientific). Effect of pH on adsorption of MB and RB by biochar was studied. The rate of adsorptions of MB and RB were observed at different concentrations of dye (10, 20, 30, 40 and 50 mg/L). Kinetic studies of adsorption were done at various concentrations of MB wherein the extent of adsorption was investigated as a function of time.

3.11. Equilibrium study

In the present study, equilibrium data were fitted by "two-parameter isotherms" including Freundlich, Langmuir, Temkin, Hurkins-Jura and Dubinin-Radushkevich (D-R) isotherms.

3.11.1. Langmuir Adsorption Isotherm

The Langmuir adsorption isotherm model is based on the assumption that there are a finite number of active sites which are homogeneously distributed over the surface of the adsorbent. These active sites have the same affinity for adsorption of a mono molecular layer and there is no interaction between adsorbed molecules [23].

Based upon these assumptions, Langmuir equation can be represented as:

$$q_e = \frac{q_m K_L C_e}{1 + K_L Ce} \qquad (3.16)$$

Langmuir adsorption parameters were determined by transforming the Langmuir equation (3.16) into linear form

$$\frac{1}{q_e} = \frac{1}{q_m} + \frac{1}{q_m K_L C_e} \qquad (3.17)$$

Where, C_e = the equilibrium concentration of adsorbate (mg/L); q_e = the amount of metal/dye adsorbed per unit mass of adsorbent at equilibrium (mg/g); q_m = maximum monolayer coverage capacity (mg/g); K_L = Langmuir isotherm constant (L/mg).

The values of q_m and K_L were calculated from the slope and intercept of the Langmuir plot of $\frac{1}{q_e}$ vs. $\frac{1}{C_e}$. When linearized the Langmuir equation, the q_e and Ce varies with each other in five different ways (like, C_e/q_e vs. C_e, $1/q_e$ vs. $1/C_e$, q_e vs.-q_e/C_e, q_e/C_e vs. q_e and $1/C_e$ vs. $1/q_e$) as reported by Huang and Shih [24].

The essential features of the Langmuir isotherm may be expressed in terms of equilibrium parameter R_L, which is a dimensionless constant referred to as separation factor or equilibrium parameter [25]. The physical significance of the factor R_L is that, the R_L value gives an idea about the shape of the isotherm which further helps to predict whether an adsorption system is "favorable" or "unfavorable".

$$R_L = \frac{1}{(1+ K_L C_o)} \qquad (3.18)$$

Where, C_o = initial concentration (mg/L); R_L value indicates the shape of the isotherm and the nature of the adsorption process.

When R_L value lies between 0 and 1 then adsorption is favorable.
If R_L is > 1, adsorption is unfavorable;
If R_L is =1, adsorption is linear;
If R_L is = 0, adsorption is irreversible.

A high value of correlation coefficient R^2 obtained from graph indicates a good agreement between the parameters and confirms the monolayer adsorption onto the adsorbent surface.

3.11.2. Freundlich Adsorption Isotherm

Freundlich adsorption isotherm is commonly used to describe the adsorption characteristics for the heterogeneous surface [22]. The adsorption isotherm is expressed by the following empirical equation

$$q_e = K_F \, C_e^{\frac{1}{n}} \qquad (3.19)$$

This can be represented in linear form as

$$l_n q_e = l_n K_F + \frac{1}{n} l_n C_e \qquad (3.20)$$

Where, K_F and $\frac{1}{n}$ are Freundlich isotherm constants related to adsorption capacity (mg/g) and sorption intensity (rate of adsorption) respectively. Moreover, the exponent $(\frac{1}{n})$ provides an indication of favorability and capacity of the adsorbent/adsorbate system [26]. The Freundlich parameter $\frac{1}{n}$ is a measure of the deviation of the adsorption from linearity. If *n* is equal to unity the adsorption is linear. This means that the adsorption sites are homogeneous (as in the Langmuir model) in energy and no interaction take place between the adsorbed species. If the value of $\frac{1}{n}$ is smaller than 1, which reflects favorable adsorption, the sorption capacity increases and new adsorption sites occur. When the value of $\frac{1}{n}$ is larger than 1, ($\frac{1}{n} \gg 1$), the adsorption bond becomes weak; and unfavorable adsorption takes place, as a result of which the adsorption capacity decreases [27].

3.11.3. Temkin Adsorption Isotherm

The Temkin adsorption isotherm assumes that the heat of adsorption decreases linearly with the sorption coverage due to adsorbent-adsorbate interactions [23]. Derivation of the equation is characterized by a uniform distribution of binding energies (up to some maximum binding energy) was carried out by plotting the q_e against $logC_e$ and the constants were determined from the slope and intercept. The model is given by the following equation [22].

$$q_e = \frac{RT}{b_T} l_n (K_T C_e) \qquad (3.21)$$

This equation can be represented in the following linear form

$$q_e = \frac{RT}{b} l_n K_T + \frac{RT}{b} l_n C_e \qquad (3.22)$$

where, $B = \frac{RT}{b}$

K_T = Temkin isotherm equilibrium binding constant (L/mg); b = Temkin isotherm constant; B = constant related to heat of sorption (J/mol); R= Ideal gas constant (8.314J/mol/ K); T= Temperature at 298 K.

3.11.4. Dubinin–Radushkevich adsorption isotherm

Dubinin-Radushkevich (D-R) isotherm is an empirical model generally applied to express the adsorption mechanism onto a heterogeneous surface [22, 28]. This adsorption isotherm is given as

$$q_e = (q_m) \exp(-B\varepsilon^2) \quad (3.23)$$

The linear form of isotherm is expressed as follows

$$l_n\, q_e = l_n(\, q_m) - (B\varepsilon^2) \quad (3.24)$$

Where, $\varepsilon = RT\ l_n\,(1 + \frac{1}{C_e})$

q_e = amount of adsorbate in the adsorbent at equilibrium (mg/g); q_m= theoretical monolayer saturation capacity of the adsorbent (mol/g); B = Dubinin–Radushkevich isotherm constant (mol^2/kJ^2)

The approach was usually applied to distinguish the physical and chemical adsorption of metal ions with its mean free energy, E per molecule of adsorbate (for removing a molecule from its location in the sorption space to the infinity) can be computed by the relationship [22].

$$E = \frac{1}{\sqrt{2B}} \quad (3.25)$$

3.11.5. Hurkins-Jura adsorption isotherm

The Hurkins-Jura adsorption isotherm can be expressed as [28]

$$q_e = \sqrt{\frac{A_H}{B_H + Log\ C_e}} \quad (3.26)$$

This can be rearranged as follows:

$$\frac{1}{q_e^2} = \frac{B_H}{A_H} - \frac{1}{A_H} \log C_e \qquad (3.27)$$

Where, A_H (mg/g) and B_H are two parameters characterizing the sorption equilibrium.

A plot of $\frac{1}{q_e^2}$ vs. $log\ C_e$ enables the determination of model parameters A_H and $B_H$from the slope and intercept. The isotherm equation accounts for multilayer adsorption. Relevant isotherm parameters (A and B) were calculated from the intercept and the slope of the Harkins-Jura plot, respectively.

3.12. Kinetic Study for adsorption

In order to investigate the controlling mechanism of adsorption processes such as mass transfer and chemical reaction, the pseudo-first-order and pseudo-second-order equations are applied to model the kinetics of adsorption.

The pseudo-first-order rate equation is given as [29]

$$\log (q_e - q_t) = \log q_e - \frac{K_{ad}}{2.303} - t \qquad (3.28)$$

Where, q_t and q_e are the amount adsorbed (mg/g) at time, t, and at equilibrium respectively. K_{ad} is the rate constant of the pseudo-first-order adsorption process (min^{-1}). Plot of $\log (q_e - q_t)$ vs. t gives the pseudo-first-order adsorption.

The pseudo-second-order kinetic relationship between sorption quantity and time can be expressed as [26]

$$\frac{t}{q_t} = \frac{1}{k q_e^2} + \frac{t}{q_e} \qquad (3.29)$$

Where, q_t and q_e are sorption quantity at time t and equilibrium respectively, k is the rate constant. Thus, a plot of $\frac{t}{q_t}$ vs. t gives the pseudo-second-order adsorption [28]. The pseudo-first-order and pseudo-second-order rate constants were determined from respective plots along with the corresponding correlation coefficients.

References:

1. Kushwah, Y. S., Mahanta, P., and Mishra, S. C. Some studies on fuel characteristics of *Mesua ferrea*. *Heat Transfer Engineering*, 29(4): 405-409, 2008.
2. Bobade, S., and Khyade, V. Detail study on the Properties of *Pongamia pinnata* (Karanja) for the Production of Biofuel. *Research Journal of Chemical Sciences*, 2(7): 16–20, 2012.
3. Eipeson, W. S., Manjunatha, J. R., Srinivas, P., and Kanya, T. S. Extraction and recovery of karanjin: A value addition to karanja (*Pongamia pinnata*) seed oil. *Industrial Crops and Products*, 32(2): 118-122, 2010.
4. Okkou, H., Naddaf, M., Alinizam, A., and Azmeh, M. F. Growth Promotion of indigenous *Scenedesmus dimorphus* strain under different conditions using stirred tank photobioreactor. *International Journal of ChemTech Research*, 8(11): 221-228, 2015.
5. Acid-insoluble lignin in wood and pulp. Reaffirmation of TAPPI Method T22 om-02, 2006. Accessed on 08/11/2017. Sait, H. H., Hussain, A., Salema, A. A., and Ani, F. N. Pyrolysis and combustion kinetics of date palm biomass using thermogravimetric analysis. *Bioresource Technology*, 118: 382-389, 2012.
6. Friedman, H. L. Kinetics of thermal degradation of char- forming plastics from thermogravimetry. Application to a phenolic plastic. Journal of Polymer Science: *Polymer Symposia*, 6(1): 183-195, 1964.
7. Ozawa, T. A new method of analyzing thermogravimetric data. *Bulletin of the Chemical Society of Japan*, 38(11): 1881-1886, 1965.
8. Flynn, J. H., and Wall, L. A. General treatment of the thermogravimetry of polymers. *Journal of Research of the National Bureau of Standards - A. Physics and Chemistry*, 70A (6): 487-523, 1966.
9. Kissinger, H. E. Variation of peak temperature with heating rate in differential thermal analysis. *Journal of Research of the National Bureau of Standards*, 57(4), 217-221, 1956.

10. Akahira, T., and Sunose, T. Method of determining activation deterioration constant of electrical insulating materials. *Research Report, Chiba Institute of Technology* (Sci Technol), 16: 22-31, 1971.
11. Sbirrazzuoli, N., Vincent, L., Mija, A., and Guigo, N. Integral, differential and advanced isoconversional methods: complex mechanisms and isothermal predicted conversion–time curves. *Chemometrics and Intelligent Laboratory Systems*, 96(2): 219-226, 2009.
12. Asphaug, S. Catalytic Hydrodeoxygenation of Bio-oils with Supported MoP-Catalysts. Master's thesis, Department of Chemical Engineering, Norwegian University of Science and Technology (NTNU), 2013.
13. Poletto, M., Zattera, A. J., Forte, M. M., and Santana, R. M. Thermal decomposition of wood: Influence of wood components and cellulose crystallite size. *Bioresource Technology*, 109: 148-153, 2012.
14. Slopiecka, K., Bartocci, P., and Fantozzi, F. Thermogravimetric analysis and kinetic study of poplar wood pyrolysis. *Applied Energy*, 97: 491-497, 2012.
15. Ceylan, S., and Topçu, Y. Pyrolysis kinetics of hazelnut husk using thermogravimetric analysis. *Bioresource Technology*, 156: 182-188, 2014.
16. Angın, D., and Tiryaki, A. E. Application of response surface methodology and artificial neural network on pyrolysis of safflower seed press cake. *Energy Sources, Part A: Recovery, Utilization, and Environmental Effects*, 38(8): 1055-1061, 2016.
17. Kılıç, M., Pütün, E., and Pütün, A. E. Optimization of Euphorbia rigida fast pyrolysis conditions by using response surface methodology. *Journal of Analytical and Applied Pyrolysis*, 110: 163-171, 2014.
18. Harvey, O. R., Kuo, L. J., Zimmerman, A. R., Louchouarn, P., Amonette, J. E., and Herbert, B. E. An index-based approach to assessing recalcitrance and soil carbon sequestration potential of engineered black carbons (biochars). *Environmental science and Technology*, 46(3), 1415-1421, 2012.
19. Pütün, E., Uzun, B. B., and Pütün, A. E. Fixed-bed catalytic pyrolysis of cotton-seed cake: effects of pyrolysis temperature, natural zeolite content and sweeping gas flow rate. *Bioresource Technology*, 97(5): 701-710, 2006.

20. Zhao, L., Cao, X., Mašek, O., and Zimmerman, A. Heterogeneity of biochar properties as a function of feedstock sources and production temperatures. *Journal of Hazardous Materials*, 256-257: 1-9, 2013.
21. Li, F., Shen, K., Long, X., Wen, J., Xie, X., Zeng, X., Liang, Y., Wei, Y., Lin, Z., Huang, W., and Zhong, R. Preparation and characterization of biochars from *Eichornia crassipes* for cadmium removal in aqueous solutions. *PloS One*, 11(2): e0148132. 2016.
22. Dada, A. O., Olalekan, A. P., Olatunya, A. M., and Dada, O. Langmuir, Freundlich, Temkin and Dubinin–Radushkevich isotherms studies of equilibrium sorption of Zn2+ unto phosphoric acid modified rice husk. IOSR *Journal of Applied Chemistry*, 3(1): 38-45, 2012.
23. Ertugay, N., and Malkoc, E. Adsorption isotherm, kinetic, and thermodynamic studies for methylene blue from aqueous solution by needles of Pinus sylvestris L. *Polish Journal of Environmental Studies*, 23(6): 1995-2006, 2014.
24. Huang, Y.T. and Shih, M.C. Effect of linearized expressions of Langmuir equations on the prediction of the adsorption of methylene blue on rice husk. *International Journal of Scientific and Research Publications,* 6(4): 549-554, 2016.
25. Zheng, H., Liu, D., Zheng, Y., Liang, S., and Liu, Z. Sorption isotherm and kinetic modeling of aniline on Cr-bentonite. *Journal of Hazardous Materials*, 167(1-3): 141-147, 2009.
26. Piccin, J. S., Dotto, G. L., and Pinto, L. A. A. Adsorption isotherms and thermochemical data of FD&C Red n 40 binding by chitosan. *Brazilian Journal of Chemical Engineering*, 28(2): 295-304, 2011.
27. Ozcan, A. S., Erdem, B., and Ozcan, A. Adsorption of Acid Blue 193 from aqueous solutions onto Na-bentonite and DTMA-bentonite. *Journal of Colloid and Interface Science*, 280(1): 44-54, 2004.
28. Kumar, P. S., and Kirthika, K. Equilibrium and kinetic study of adsorption of nickel from aqueous solution onto bael tree leaf powder. *Journal of Engineering Science and Technology*, 4(4): 351-363, 2009.

29. Ho, Y. S., and Ofomaja, A. E. Pseudo-second-order model for lead ion sorption from aqueous solutions onto palm kernel fiber. *Journal of Hazardous Materials*, 129(1): 137-142, 2006.